Analysis of a Queueing Model for Energy Storage Systems with Self-discharge

MAJID RAEIS, ALMUT BURCHARD, and JÖRG LIEBEHERR, University of Toronto, Canada

This article presents an analysis of a recently proposed queueing system model for energy storage with discharge. Even without a load, energy storage systems experience a reduction of the stored energy through *self-discharge*. In some storage technologies, the rate of self-discharge can exceed 50% of the stored energy per day. We consider a queueing model, referred to as *leakage queue*, where, in addition to an arrival and a service process, there is a leakage process that reduces the buffer content by a factor γ $(0 < \gamma < 1)$ in each time slot. When the average drift is positive, we discover that the leakage queue operates in one of two regimes, each with distinct characteristics. In one of the regimes, the stored energy always stabilizes at a point that lies below the storage capacity, and the stored energy closely follows a Gaussian distribution. In the other regime, the storage system behaves similar to a conventional finite capacity system. For both regimes, we derive expressions for the probabilities of underflow and overflow. In particular, we develop a new martingale argument to estimate the probability of underflow in the second regime. The methods are validated in a numerical example where the energy supply resembles a wind energy source.

Q1

CCS Concepts: • **Mathematics of computing → Stochastic processes**;

Additional Key Words and Phrases: Queueing theory, exponential martingale, energy storage

ACM Reference format:
Majid Raeis, Almut Burchard, and Jörg Liebeherr. 2020. Analysis of a Queueing Model for Energy Storage Systems with Self-discharge. *ACM Trans. Model. Perform. Eval. Comput. Syst.* 5, 3, Article 14 (October 2020), 26 pages.
https://doi.org/10.1145/3422711

14

1 INTRODUCTION

With their ability to absorb the intermittency and uncertainty in renewable energy generation, energy storage systems facilitate the integration of renewable energy sources into the grid. There exists a wide variety of energy storage technologies, each offering a tradeoff with regards to storage capacity per unit of volume (energy density), delivered power per unit of volume (power density), scalability, and other considerations [15]. For instance, compressed air energy storage systems have a high capacity but a low power density, which makes them suitable for long-term storage applications that do not need a fast response time. Due to the generally high cost of energy storage technologies—the price of energy storage can be thousands of dollars per kilowatt hour—the economic viability of an energy storage system crucially depends on properly dimensioning the

Q2

Authors' addresses: M. Raeis, A. Burchard, and J. Liebeherr, University of Toronto, Toronto, Ontario, Canada; emails: m.raeis@mail.utoronto.ca, almut@math.toronto.edu, jorg@ece.utoronto.ca.

2376-3639/2020/10-ART14 $15.00
https://doi.org/10.1145/3422711

storage size.[1] Over-provisioning of the storage system unnecessarily increases costs, while under-provisioning may render it ineffective. The need for tools to dimension energy storage systems has motivated the development of analytical methods. By modelling energy storage systems as finite capacity queueing systems with stochastic arrivals (energy supply) and departures (energy demand), the vast queueing theory literature becomes available to the problem of storage sizing. However, a closer inspection reveals that queueing analysis is not automatically a good fit for energy storage systems. For one, arrivals and departures in queueing theory are often expressed as point processes that track arrival and departure events. Energy supply and demand, however, are better characterized by fluid-flow processes. Also, many queueing theory methods were developed for job shop manufacturing and communication networks, where buffer provisioning is primarily concerned with preventing overflows. There, it is generally required that the average service rate exceeds the average arrival rate. Differently, in energy storage the overriding concern is the prevention of buffer underflows ("empty batteries"). Here, it is generally required that the average arrival rate exceeds the average service rate.

Different from systems usually analyzed by queueing theoretic methods, the stored energy may shrink over time even when the system is inactive. The rate of leakage of the stored energy, referred to as *self-discharge*, may be the result of chemical reactions, loss of thermal or kinetic energy, and other factors. It can be as low as 1% of the total charge per month for lithium-ion batteries [16] and may exceed 50% per day for flywheels [27]. Interestingly, there is no queueing analysis in the literature that accounts for the impact of self-discharge. The lack of analytical models was made evident in recent performance studies of energy storage [20, 21, 24, 25, 55, 60], which resorted to optimization methods when accounting for self-discharge. The main complication of the performance analysis is that self-discharge adds another process that runs concurrently with the conventional arrival (load) and service (demand) processes. Since the quantity of self-discharge depends on the amount of stored energy, the self-discharge rate is not an independent process, but is coupled to the arrival and service processes.

This article presents the first analytical study of the dynamics of queueing systems that model energy storage systems with self-discharge. The analysis enables us to address pertinent questions in energy storage. For example, how does the self-discharge process interact with the processes for energy supply and demand? Are there parameter regions where undesirable events such as overflows and underflows rarely occur? We address these questions by considering a queueing model, referred to as *queue with leakage* or *leakage queue*, where supply and demand are governed by stochastic processes and, additionally, in each time slot, the content of the queue is reduced by a factor γ, with $0 < \gamma < 1$. Since we want to study scenarios where storage underflows are rare, we assume that the average supply exceeds the average demand, resulting in a drift that is on average positive.

Under these assumptions, we make several contributions towards a queuing theoretic analysis of the leakage queue. We provide a closed-form expression for the backlog at the leakage queue. It turns out that a leakage queue with finite capacity has parameter regimes with distinct behaviors. In one of the regimes, the backlog stabilizes at a level well below its capacity, with the result that both underflows and overflows are rare events. We find that the distribution of the stored energy in this regime is close to (and in the limit exactly) Gaussian. For the general case, we derive bounds on overflow and underflow probabilities using a novel analysis based on exponential martingales.

[1] In addition to the price of acquisition, the cost of energy storage also takes into account other factors such as the number of recharge cycles over the lifetime of a unit, the amount of energy that can be withdrawn in a single recharge cycle (depth of discharge), and ancillary costs.

As a queueing model, the leakage queue does not serve as a high-fidelity model for particular storage technologies. It considers a minimalist system model that only leaves the input, output, and leakage processes in place to isolate the self-discharge effects to a maximum degree. The model does not account for the potentially complex interactions between users and utilities in demand-side management. The queueing analysis is further simplified by assuming independent arrival and service processes. This puts the focus of the analysis on the dependencies introduced by the leakage process. A relaxation of the independence assumption appears feasible, but will require substantial additional effort.

The analysis and findings in this article may be useful in other application areas. For example, in data networks, buffers with leakage have appeared as a mechanism to prevent network congestion. A group of techniques, referred to as active queue management [3, 19], intentionally drops traffic in output buffers at packet with a given probability switches to mitigate network congestion. If probabilistic dropping of traffic arrivals is viewed as a form of leakage, there is a striking resemblance to the leakage queue. Note that the amount of leakage in energy storage systems is a *system parameter* that depends on the storage technology and environmental factors. Differently, leakage that is enforced by a network control algorithm is a *design parameter* that is set to achieve a certain behavior. In fact, the observed self-stabilization in the leakage queue may be related to the stabilizing effect of Additive Increase–Multiplicative Decrease (AIMD) methods [28] and Random Early Detection [19] in network congestion control. Generalizing the leakage queue analysis to other application areas awaits future investigation.

The remainder of the article is structured as follows: In Section 2, we discuss the literature on the analysis of energy storage systems. In Section 3, we explore the dynamics of queueing systems with leakage. In Section 4, we establish the stability of the leakage queue under a broad set of assumptions. In Section 5, we present two analytical approaches, each applicable to a specified regime of parameters, for deriving overflow and underflow probabilities. In Section 6, we evaluate the analysis for an example with random processes that mimic the behavior of a renewable energy source. We present conclusions in Section 7.

2 RELATED WORK

Energy storage plays a major role in many aspects of the smart grid, and there is an extensive literature on the analysis of energy storage systems. The electrical grid requires that power generation and demand load are continuously balanced. This becomes more involved with time-variable renewable energy sources and storage systems absorbing the variations from such sources. Smart grid approaches that take the perspective of a utility operator are concerned with placement, sizing, and control of energy storage systems, with the goal to optimally balance power [50–52], reduce power generation costs [54], or control operational costs [34]. Works in this area are frequently formulated as optimal control or optimization problems, with the objective to devise distributed algorithms that achieve a desired operating point.

Demand-side management [22] takes the perspective of an energy user and broadly refers to measures that encourage users to become more energy-efficient. As one form of demand-side management, demand response refers to methods for short-term reductions in energy consumption. By creating incentives to users, demand response seeks to match elastic demands with fluctuating renewable energy sources. In References [37, 47], demand response is posed as a utility maximization problem where dynamic pricing incentivizes individual users to benefit the overall system. Studies on demand response apply a wide range of methods, from coordination between appliances [42], bounds on prediction errors [38], and game-theoretic approaches [39].

Performance analysis of energy storage systems intends to support the dimensioning of storage by providing metrics such as overflow and underflow probabilities and the amount of stored energy

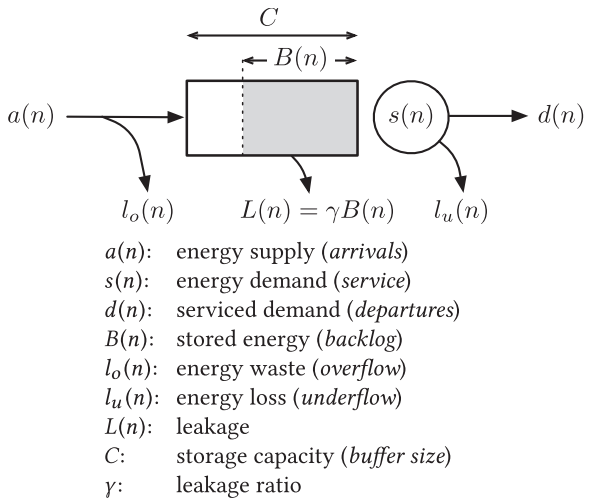

Fig. 1. Queueing model of energy storage system.

in the steady state. Since detailed models of the circuit or electrochemical processes in an energy storage system, as given in References [11, 30, 46], are not analytically tractable, energy storage systems are generally described by abstract models. Differential or difference equations have been used for detailed descriptions of the evolution in lithium-ion batteries [30] and flywheels [20, 21]. The suitability of queueing theory for analyzing the dynamics of energy storage has been pointed out in Reference [2]. Interestingly, queueing theory was applied in the 1960s for analyzing storage properties of water reservoirs [13, Chapter 3.5], and the fluid-flow analysis of queueing systems was known as *dam theory* [43]. More recently, a fluid-flow queueing analysis for rechargeable batteries was presented in Reference [29]. A concise presentation of the state-of-the-art of fluid-flow queueing analysis is found in Reference [9].

More recently, a fluid-flow interpretation of queueing theory, known as *network calculus* [35], has been applied to energy storage systems. A deterministic analysis has been used in Reference [36] to devise battery charging schedules that prevent batteries from running empty. Stochastic extensions of the network calculus have been applied to analyze energy storage in the presence of random, generally Markovian, energy sources [49, 56, 59]. In these works, the evolution of the stored energy is expressed as the time-dependent backlog in the finite capacity queueing system from Reference [14]. Recent studies [21, 24, 25, 55, 60] have improved the fidelity of energy storage models by considering factors such as limited charging and discharging rates, charging and discharging inefficiencies, as well as self-discharge. In Reference [24], the self-discharge is modeled by a constant rate function, whereas the other works [21, 25, 55, 60] use a proportional leakage ratio as described in Section 1. Since queueing systems for energy storage systems with proportional self-discharge could not be solved analytically, the existing analyses resort to simulation and optimization methods. These provide numerical solutions, but do not easily give insight into parameter regimes and basic tradeoffs.

3 A QUEUEING MODEL FOR ENERGY STORAGE WITH SELF-DISCHARGE

We model an energy storage system as a finite queueing system, as shown in Figure 1. The arrivals to the system consist of a time-varying energy supply from energy sources, the service process consists of the time-varying energy demand from customers, and the departures are the serviced demand. The stored energy and capacity, which correspond to the backlog and capacity in a

conventional queueing system, are measured in watt hours (Wh). In the following, we will use the terms *supply* and *arrivals*, as well as *demand* and *service,* synonymously. As a convention, we will employ queueing theory terminology when making comparisons to other queueing systems.

3.1 Dynamics of the Leakage Queue

For the purpose of the analysis, we assume that the energy processes are discrete-time, fluid flow random processes, where we consider deterministic processes as a special case. The energy supplied when the storage is at capacity is considered wasted, and demand to an empty storage is considered lost. We use $a(n)$, $s(n)$, and $d(n)$ to denote the energy supply, energy demand, and serviced demand, respectively, in time slot n, measured in Wh. We define the *drift* or *net charge* of the system in slot n, denoted by $\delta(n)$, as the difference

$$\delta(n) = a(n) - s(n).$$

The amount of energy stored at time slot n, denoted by $B(n)$ and referred to as stored energy, corresponds to the backlog in the usual terminology of queueing theory. Alternative terms in the energy storage literature are energy content, state of charge, or battery load. The maximum amount of stored energy, referred to as storage capacity, is denoted by C.

We assume that the queue has a fixed self-discharge ratio γ with $0 < \gamma < 1$, which we will refer to as leakage ratio. The interpretation is that the stored energy at time n, $B(n)$, shrinks to $(1-\gamma)B(n)$ by time slot $n+1$. The amount of leaked storage in time slot n is given by the leakage process $L(n) = \gamma B(n)$. The case $\gamma = 0$ refers to a system without self-discharge. Since the leakage ratio frequently appears in the form $1-\gamma$, we define the complementary leakage ratio $\bar{\gamma}$ as $\bar{\gamma} = 1-\gamma$. The energy evolution of the storage system can be described in terms of a recursive equation [25, 55] by

$$B(n) = \min\{[\bar{\gamma}B(n-1) + \delta(n)]^+, C\}, \tag{1}$$

where we use the notation $[x]^+ = \max\{x, 0\}$. We refer to a queueing system with this dynamics as a *queue with leakage* or *leakage queue*. Descriptions of energy storage systems generally use a fixed self-discharge ratio, even though the self-discharge may depend on the amount of stored energy, temperature, or other factors. Here, the fixed self-discharge ratio represents a long-term average [27].

The leakage queue described above is distinct from other queueing systems where admittance, service, or sojourn time are functions of the system state, in particular, the extensively studied reneging and balking queues [1, 6]. In a balking queue, an arrival refuses to enter the queue with a probability that depends on the current backlog. In a reneging queue, a customer leaves the queue if its waiting time exceeds a (generally randomly determined) threshold. In the special case where the threshold of a customer follows an exponential distribution, the reneging queue has a superficial resemblance with the leakage queue, in that customers leave the system at a fixed exponential rate. However, the leakage queue is not simply a fluid-flow limit of the reneging queue. In a naive fluid-flow limit, where the service times of arrivals are taken to zero so the random reneging process becomes a non-random constant-rate leakage process, the arrival and service processes also converge to constant-rate functions. Non-trivial fluid-flow limits of reneging queues are known only in the heavy-traffic regime where the reneging rate goes to zero and the backlog becomes very large [57]. Such limits are not relevant for a leakage queue of finite capacity. It is also feasible to relate the leakage queue to a queueing system that admits negative customers [23, 26]. The difference between the leakage queue and a queue with negative customers is that the leakage process in the former has a multiplicative (proportional) impact on the backlog, whereas the arrival process of negative customers in the latter has an additive (subtracting) impact. In principle, it is

feasible to express the leakage process in terms of an arrival process of (fluid) negative customers; however, this arrival process is quite complex, as it depends on the queue occupancy.

When time units are expressed in hours, a self-discharge of 5% per day for a full battery corresponds to a leakage ratio of $\gamma = 0.0021$. This holds, since the leakage in a day is $1 - \bar{\gamma}^{24}$. Likewise, we have the correspondences

$$\begin{aligned} 10\% \text{ discharge per day} &\sim \gamma = 0.0044, \\ 20\% \text{ discharge per day} &\sim \gamma = 0.0093, \\ 50\% \text{ discharge per day} &\sim \gamma = 0.0285. \end{aligned}$$

Note that the leakage ratio depends on the length of the time slot.

We use $l_u(n)$ and $l_o(n)$ to denote the underflow and overflow processes, respectively, at the storage system. In the context of energy storage, $l_u(n)$ is often referred to as the *loss of power* and $l_o(n)$ is referred to as the *waste of power*. The processes are given by

$$\begin{aligned} l_u(n) &= [-\bar{\gamma}B(n-1) - \delta(n)]^+, \\ l_o(n) &= [\bar{\gamma}B(n-1) + \delta(n) - C]^+. \end{aligned} \tag{2}$$

The recursion relation in Equation (1) can be refined to incorporate other pertinent features of an energy storage system [24]. We define the bivariate process $\Delta_\gamma(m,n)$ as

$$\Delta_\gamma(m,n) = \sum_{k=m+1}^{n} \bar{\gamma}^{n-k}\delta(k).$$

Our first result, presented in the next theorem, is an explicit non-recursive expression for the stored energy in a queue with leakage. The theorem extends the backlog equation by Cruz and Liu for finite capacity queues [14] to leakage queues.

Theorem 3.1. *Let $B(n)$ be the stored energy in a leakage queue with finite capacity C and leakage ratio γ, as in Equation (1). Then*

$$B(n) = \min_{0\le m\le n}\Big\{\max_{m\le j\le n}\{\bar{\gamma}^{n-m}C_m\mathbb{1}_{j=m} + \Delta_\gamma(j,n)\}\Big\}, \tag{3}$$

where $\mathbb{1}_{j=m}$ is the indicator function that evaluates to 1 if $j = m$, and to 0 otherwise, and C_m is defined as

$$C_m = \begin{cases} B(0) & \text{if } m = 0, \\ C & \text{if } m > 0. \end{cases}$$

Equation (3) implies that the effect of the initial charge $B(0)$ vanishes as time increases. By taking $C \to \infty$, we immediately get for a leakage queue with infinite capacity that

$$B(n) = \max_{0\le j\le n}\{\bar{\gamma}^n C_0\mathbb{1}_{j=0} + \Delta_\gamma(j,n)\}.$$

Proof. We first argue that

$$B(n) \le \min_{0\le m\le n}\Big\{\max_{m\le j\le n}\{\bar{\gamma}^{n-m}C_m\mathbb{1}_{j=m} + \Delta_\gamma(j,n)\}\Big\}. \tag{4}$$

Let m be an arbitrary time slot with $0 \le m \le n$. If $B(j) > 0$ for all j with $m < j \le n$, then

$$B(j) \le \bar{\gamma}B(j-1) + \delta(j), \quad \text{for } m < j \le n,$$

which implies

$$B(n) \le \bar{\gamma}^{n-m}B(m) + \Delta_\gamma(m,n).$$

Otherwise, let j be the last time slot with $m < j \le n$ such that $B(j) = 0$. Then

$$B(n) \le \Delta_\gamma(j,n).$$

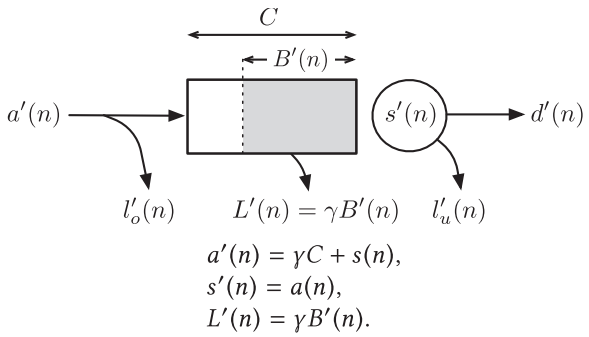

Fig. 2. Model of the dual system.

In either case, since $B(m) \leq C_m$, it follows that

$$B(n) \leq \max_{m \leq j \leq n} \{\bar{\gamma}^{n-m} C_m \mathbb{1}_{j=m} + \Delta_\gamma(j,n)\}. \tag{5}$$

Since m was arbitrary, this establishes Equation (4).

For the reverse inequality, it suffices to find one value of m that produces equality in Equation (5). Choose $m = 0$ if $B(j) < C$ for all $j = 1, \ldots, n$. Otherwise, choose m to be the index of the last time slot up to n with $B(m) = C$. Since no overflow occurs in time slots $j = m+1, \ldots, n$, the recursion in Equation (1) yields

$$B(j) = [\bar{\gamma} B(j-1) + \delta(j)]^+, \quad \text{for } m < j \leq n.$$

Since $B(m) = C_m$ by the choice of m, it follows that Equation (5) holds with equality. □

3.2 The Dual System

Numerous analytical methods are available for estimating the overflow probability at a buffered link. These methods were developed for applications of queueing theory in telecommunications and manufacturing, e.g., Reference [31]. In some application areas, however, such as multimedia streaming and energy storage, underflow is a more serious concern than overflow. By developing dual models where the roles of underflow and overflow events are switched, the existing know-how for computing overflow probabilities can be leveraged for the computation of underflow probabilities [2, 8]. We follow this approach by deriving a dual system for a leakage queue. Since the dual system is not a physical system, we resort to conventional queueing terminology and talk about arrivals, service, and backlog.

We refer to the leakage queue in Figure 1 as the original system. The dual system is a leakage queue with the same capacity C and leakage ratio γ. Arrivals and service at the dual system, denoted by $a'(n)$ and $s'(n)$, are defined as $a'(n) = \gamma C + s(n)$ and $s'(n) = a(n)$, with $\delta'(n) = a'(n) - s'(n)$. We denote by $B'(n)$ the backlog process of the dual system. The overflow and underflow processes of the dual system, denoted by $l'_o(n)$ and $l'_u(n)$, are as in Equation (2), where we replace $\delta(n)$ by $\delta'(n)$ and $B(n)$ by $B'(n)$. Figure 2 illustrates the queueing model of the dual system. With this definition, the backlog $B'(n)$ of the dual system satisfies the recursion

$$B'(n) = \min\left\{[\bar{\gamma} B'(n-1) + \delta'(n)]^+, C\right\}. \tag{6}$$

Duality of the original and the dual system is established by the following lemma.

Lemma 3.2. *Given a queue with leakage as shown in Figure 1 and the dual system shown in Figure 2. If $B(0) + B'(0) = C$, then the backlog in the original system and the dual system satisfy*

$$B(n) + B'(n) = C$$

for all $n > 0$.

From the lemma it follows immediately that $l'_o(n) = l_u(n)$ and $l'_u(n) = l_o(n)$, as long as the dual system is properly initialized. Hence, we can obtain the underflow probability in the original system by computing the overflow probability in the dual system.

Proof. We proceed by induction. The base case is covered by the assumption that $B(0) + B'(0) = C$. For the inductive step, suppose that $B(n-1) + B'(n-1) = C$ for some $n > 0$. In particular, $0 \leq B'(n-1) \leq C$. We rewrite Equation (6) in terms of $C - B'(n)$ and apply the identity

$$C - \min\left\{[x]^+, C\right\} = \min\left\{[C-x]^+, C\right\}$$

to obtain

$$\begin{aligned} C - B'(n) &= C - \min\left\{[\bar{\gamma}B'(n-1) + \delta'(n)]^+, C\right\} \\ &= \min\left\{[C - \bar{\gamma}B'(n-1) - \delta'(n)]^+, C\right\} \\ &= \min\left\{[\bar{\gamma}(C - B'(n-1)) + \gamma C - \delta'(n)]^+, C\right\}. \end{aligned}$$

Since $C - B'(n-1) = B(n-1)$ by the inductive hypothesis, and $\gamma C - \delta'(n) = \delta(n)$, it follows that

$$C - B'(n) = \min\left\{[\bar{\gamma}B(n-1) + \delta(n)]^+, C\right\}.$$

We conclude with Equation (1) that $C - B'(n) = B(n)$. □

We exploit the dual system to obtain an alternative expression for the backlog.

Corollary 3.3. *The backlog in a leakage queue with capacity C and leakage ratio γ is given by*

$$B(n) = \max_{0 \leq m \leq n} \left\{ \min_{m \leq j \leq n} \{\bar{\gamma}^n B(0) \mathbb{1}_{j=m=0} + \bar{\gamma}^{n-j} C \mathbb{1}_{j>m} + \Delta_\gamma(j,n)\} \right\}.$$

Proof. Write $B(n) = C - B'(n)$ and apply Theorem 3.1 to the dual system. □

3.3 The Two Regimes of the Leakage Queue

In this subsection, we make observations that will prove crucial for the analysis of leakage queues. Throughout, we will work with a drift $\delta(n)$ that is positive on average, since the system will be frequently empty otherwise. We find that the leakage queue operates in two regimes with fundamentally different behaviors. In one regime, the stored energy is stable at a point below the storage capacity. Here, the leakage queue behaves similarly to a reference system with simpler properties that admits an exact solution. In the other regime, the stored energy is generally close to the capacity. Here, the leakage queue behaves similarly to a conventional finite capacity queueing system in overload.

We illustrate the different regimes with the aid of a numerical example drawn from an energy storage system with a photo-voltaic (PV) energy source and constant demand. We use the PV energy generation for a residential rooftop system, which is based on an hourly dataset of the typical solar irradiance in Los Angeles for the month of July [40]. The resulting solar energy is calculated with the System Advisor Model (SAM) software [41], where solar panels are scaled so the average energy supply per hour is 1 kWh. The demand per hour is assumed to be constant and set to 0.8 kWh, which is 80% of the supply. This is approximately the average hourly power consumption per household in New Zealand [58].

For calibration, we first consider a system without leakage, that is, $\gamma = 0$. In Figure 3, we depict the energy content for systems with storage capacity $C = 10$ kWh and $C = 40$ kWh, where we assume that the storage is initially empty. Observe that the data captures the diurnal pattern of

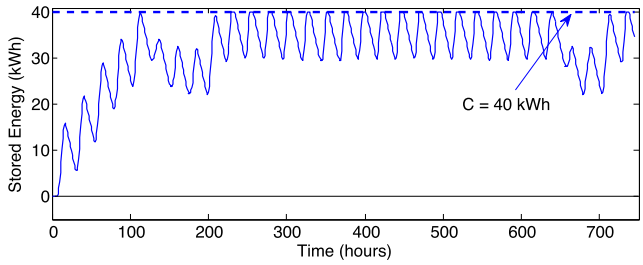

(a) $C = 40$ kWh.

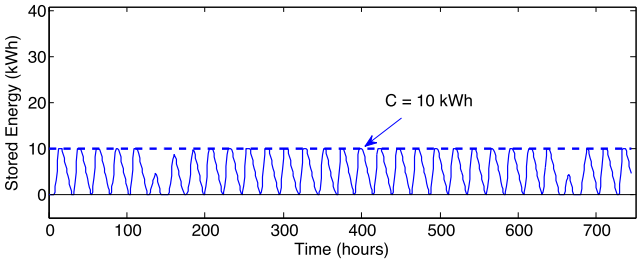

(b) $C = 10$ kWh.

Fig. 3. Stored energy **without self-discharge** with solar power supply. Since the supply (arrivals) on average exceed the demand (service), the filling level always stays close to the capacity C.

solar energy. As expected, once the storage fills up, the stored energy stays always close to the storage capacity.

Before we discuss how the outcome changes in the presence of self-discharge, we introduce a reference system that differs from the leakage queue in two ways. First, the reference system has infinite storage capacity ($C = \infty$). Second, the stored energy is allowed to take negative values, where a negative occupancy can be thought of as an energy deficit. The dynamics of the stored energy in the reference system, denoted by B^r, simplify to

$$B^r(n) = \bar{\gamma} B^r(n-1) + \delta(n). \tag{7}$$

The solution of this recursion is $B^r(n) = \bar{\gamma}^n B(0) + \Delta_\gamma(m,n)$. If $\delta(n)$ describes a stationary process with $\delta(n) =_{\mathcal{D}} \delta$ for all n, where "$=_{\mathcal{D}}$" indicates equality in distribution, then the expected value is

$$\mathrm{E}[B^r(n)] = \bar{\gamma}\mathrm{E}[B^r(n-1)] + \mathrm{E}[\delta].$$

If there exists a steady state for B^r, then, for $n \to \infty$, the expected stored energy, denoted by $\mathrm{E}[B^r]$, is given by

$$\mathrm{E}[B^r] = \lim_{n\to\infty} \mathrm{E}[B^r(n)] = \frac{\mathrm{E}[\delta]}{\gamma}. \tag{8}$$

In the next section, we will prove that $B^r(n)$ converges to a steady state, with expected value $\mathrm{E}[B^r]$.

We now re-compute the numerical example from Figure 3 with a leakage ratio of $\gamma = 0.0093$ (20% leakage daily). With the given supply and demand, we obtain that $\mathrm{E}[B^r] = 21.5$ kWh, where, for the dataset, $\mathrm{E}[B^r]$ is the average drift divided by γ. Figure 4 shows the stored energy for the reference system and the finite capacity leakage queue. Note that the reference system initially takes negative values for $B^r(n)$. In Figure 4(a), where $C > \mathrm{E}[B^r]$, the stored energy in the reference system tracks the energy in the finite capacity leakage queue with a high degree of accuracy. In Figure 4(b), we show the results for $C < \mathrm{E}[B^r]$. Here, the stored energy in the finite capacity leakage queue is very

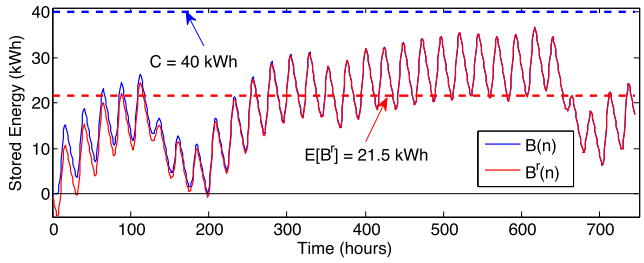

(a) $C = 40$ kWh.

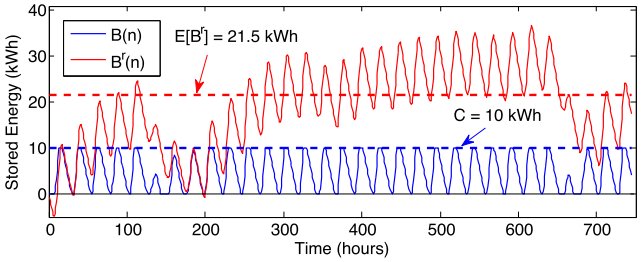

(b) $C = 10$ kWh.

Fig. 4. Stored energy with **20% self-discharge per day** with solar power supply. In (a), when $C > \mathrm{E}[B^r]$, the stored energy $B(n)$ (blue line) remains well below the capacity. In (b), where $C < \mathrm{E}[B^r]$, the stored energy stays close to the capacity. The stored energy $B^r(n)$ of the reference system (red line) tracks the actual stored energy well in (a), but not in (b).

different from that of the reference system. In fact, the dynamics of the leakage queue resemble that of the finite capacity queue without leakage (shown in Figure 3(b)).

In the next sections, we will establish that our observations in the numerical example extend to other supply and demand distributions. It turns out that all leakage queues with $\gamma > 0$ operate in one of two modes, which we will refer to as *capacity-dominated regime* and *leakage-dominated regime*, with very different characteristics.

- **Leakage-dominated regime ($C > \mathrm{E}[B^r]$):** This regime, illustrated in Figure 4(a), is characterized by an average stored energy below the storage capacity. This is unlike a conventional finite capacity queueing system (with $\gamma = 0$), where the storage is full or close to full for $\mathrm{E}[\delta] > 0$.
- **Capacity-dominated regime ($C < \mathrm{E}[B^r]$):** In this regime, illustrated in Figure 4(b), the stored energy is generally close to the capacity C, which necessarily results in a high probability of overflow. The system behaves similarly to a conventional finite capacity queueing system without leakage.

We will study the regimes in detail in Section 5, where we find that we must use different analysis methods for each regime.

An interesting property of leakage queues is that increasing the storage capacity much beyond $\mathrm{E}[B^r]$ does not result in significant benefits. To emphasize this, we consider the same dataset as used for Figures 3 and 4 and compute the average stored energy as a function of the storage capacity. In Figure 5, we show the results for a daily self-discharge of 0%, 20%, and 50%. Without self-discharge, the average stored energy is always close to the capacity. With positive self-discharge, however, the average storage approaches a constant even as the capacity goes to infinity. The

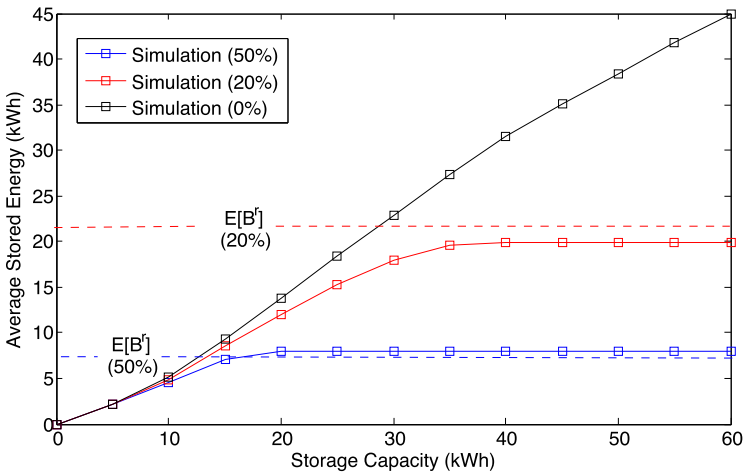

Fig. 5. Average stored energy with self-discharge per day of 0%, 20%, or 50% with solar power supply.

value of this constant is close to the stored energy in the reference system. To our knowledge, this feature of energy storage systems with self-discharge has not been reported previously.

So far, our observations of the stability of the leakage queue and the characterization of the leakage-dominated regime by the reference system are limited to the depicted dataset. In the next sections, we will corroborate our empirical findings for general random processes.

4 STABILITY AND CONVERGENCE

In this section, we prove that the leakage queue defined by Equation (1) converges for $0 < \gamma < 1$ to a unique steady state as $n \to \infty$. The drift $\delta(n)$ for $n = 0, 1, \ldots$ is assumed to be an i.i.d. sequence of random variables of finite expectation $\mathrm{E}[\delta]$. Assuming that $\mathrm{E}[\delta] > 0$, we characterize the steady-state distribution of the stored energy, B, in terms of the steady state of the reference system B^r and the capacity C. In the leakage-dominated regime, where $C > E[B^r]$, we prove that the steady state is close to that of the reference system. In the capacity-dominated regime, where $C < E[B^r]$, the expected drift in the dual system is negative. The steady state resembles that of a stable queue without leakage.

4.1 Stability

A leakage queue of finite capacity C is stable by definition, since $0 \le B(n) \le C$ for all $n \ge 0$. We will derive another bound on the distribution of $B(n)$ that does not depend on the capacity C. This bound explains the stability of the buffer content that we observed in the leakage-dominated regime in Figures 4(a) and 5.

By the recursive definition from Equation (1), we have that $B(n) \le \bar{\gamma} B(n-1) + [\delta(n)]^+$. Solving the recursion, and then using the i.i.d. assumption on the drift, we obtain

$$\begin{aligned} B(n) &\le \bar{\gamma}^n B(0) + \sum_{m=1}^{n} \bar{\gamma}^{n-m} [\delta(m)]^+ \\ &=_{\mathcal{D}} \bar{\gamma}^n B(0) + \sum_{m=0}^{n-1} \bar{\gamma}^m [\delta(m)]^+ =: Y(n). \end{aligned}$$

In particular,

$$\mathrm{E}[B(n)] \leq \mathrm{E}[Y(n)] = \bar{\gamma}^n B(0) + \frac{1-\bar{\gamma}^n}{\gamma}\mathrm{E}\Big[[\delta]^+\Big].$$

As $n \to \infty$, the random variables converge to

$$Y := \sum_{m=0}^{\infty} \bar{\gamma}^m [\delta(m)]^+ .$$

By monotone convergence, Y has finite mean, and is almost surely finite. By construction, $Pr(B(n) > x) \leq Pr(Y > x)$ holds for all $n \geq 0$. Thus, Y provides a bound that does not depend on C. The bound improves upon C when $C \gg E[B_r]$. For the reference system, a similar argument, using dominated convergence, shows that $B^r(n)$ converges in distribution to

$$B^r := \sum_{m=0}^{\infty} \bar{\gamma}^m \delta(m). \tag{9}$$

Since this series converges absolutely almost surely, the reference system is stable as well. We will refer to B^r as the steady-state distribution of the reference system. Note that the expected value of Equation (9) agrees with Equation (8), justifying our earlier use of the notation $\mathrm{E}[B^r]$.

4.2 Convergence to Steady State

We next show that the stored energy in a leakage queue converges in distribution to a steady state.

Theorem 4.1. *Let $\delta(n)$ be an i.i.d. sequence of finite mean, $C > 0$, and $0 < \gamma < 1$. Then the stored energy $B(n)$ in a queue with leakage ratio γ, storage capacity C, and drift $\delta(n)$ converges in distribution to a steady state that does not depend on the initial condition.*

The key observation is that Equation (1) defines a contraction in a suitable metric on the space of probability distributions. Given two random variables X_1, X_2, with cumulative distribution functions (CDF) $F_1(x) = Pr(X_1 \leq x)$ and $F_2(x) = Pr(X_2 \leq x)$. Their Kantorovich-Rubinstein distance is defined by

$$d(F_1, F_2) = \int_{-\infty}^{\infty} |F_1(x) - F_2(x)|\, dx.$$

With a slight abuse of notation, we write $d(X_1, X_2)$ in place of $d(F_1, F_2)$ for the Kantorovich-Rubinstein distance between the distributions of X_1 and X_2. The following technical lemma provides the necessary estimates. The proof is given in the Appendix.

Lemma 4.2. *Let X_1 and X_2 be random variables of finite mean. Then*

1. *$d(\alpha X_1, \alpha X_2) = \alpha d(X_1, X_2)$ for every $\alpha > 0$.*
2. *$d([X_1]^+, [X_2]^+) \leq d(X_1, X_2)$.*
3. *$d(\min\{X_1, C\}), \min\{X_2, C\}) \leq d(X_1, X_2)$ for every $C \in \mathbb{R}$.*
4. *$d(X_1 + Y, X_2 + Y) \leq d(X_1, X_2)$ for every random variable Y of finite mean that is independent of X_1 and X_2.*

Proof of Theorem 4.1. Let Ψ be the transformation that maps the distribution of $B(n-1)$ to the distribution of $B(n)$ according to Equation (1). Explicitly,

$$\Psi(X) =_{\mathcal{D}} \min\Big\{[\bar{\gamma}X + \delta]^+, C\Big\}, \tag{10}$$

where δ is independent of X. By Lemma 4.2,

$$\begin{aligned} d(\Psi(X_1), \Psi(X_2)) &\leq d(\bar{\gamma}X_1, \bar{\gamma}X_2) \\ &= \bar{\gamma} d(X_1, X_2). \end{aligned}$$

By Banach's contraction mapping theorem, Ψ has a unique fixed point, which we denote by B. Moreover, by induction,

$$d(B(n), B) \leq \bar{\gamma}^n d(B(0), B),$$

proving convergence to the steady state. □

The last step of the proof allows us to strengthen Theorem 4.1.

Corollary 4.3. *The convergence of $B(n)$ to the steady state in Theorem 4.1 occurs exponentially fast.*

The same argument as in Theorem 4.1 shows the convergence of a leakage queue of infinite capacity to its steady state. The only change is that Equation (10) should be replaced by $\Psi(X) =_{\mathcal{D}} [\bar{\gamma}X + \delta]^+$.

The proof of the theorem also yields an estimate for the distance of the steady state in the leakage queue from the steady state of the reference system (see Equation (9)). The estimate, given in the next corollary, is proved in the Appendix.

Corollary 4.4. *The steady-state distributions of the stored energy in the leakage queue and the reference system satisfy*

$$d(B, B^r) \leq \frac{1}{\gamma}\left(\int_{-\infty}^{0} Pr(B^r \leq x)\,dx + \int_{C}^{\infty} Pr(B^r > x)\,dx\right).$$

5 PROBABILISTIC BOUNDS

In this section, we quantify the underflow and overflow probabilities $Pr(l_u > 0)$ and $Pr(l_o > 0)$ at the leakage queue. Based on Section 3, we expect the reference system to provide a good approximation for the leakage queue in the leakage-dominated regime where the storage capacity is large enough to absorb random variations of power supply and demand. For the capacity-dominated regime, we offer a separate martingale analysis. As in Section 4, we assume that the drift $\delta(n)$ is an i.i.d. process with finite mean. We now additionally assume that $\delta(n)$ has finite variance.

5.1 Gaussian Analysis

In Section 4, we showed that the stored energy in the reference system $B^r(n)$ has a unique steady state, given by Equation (9). In the special case where $\delta(k)$ follows a Gaussian distribution, the reference system B^r is also Gaussian, with mean and variance in the steady state given by

$$\mathrm{E}[B^r] = \frac{\mathrm{E}[\delta]}{\gamma}, \qquad \mathrm{Var}[B^r] = \frac{\mathrm{Var}[\delta]}{1-\bar{\gamma}^2}. \tag{11}$$

Let B be the steady state of the stored energy in the corresponding leakage queue. If $C > E[B^r]$, we expect the stored energy B to be well-approximated by B^r (see Corollary 4.4). In particular, underflow and overflow probabilities should be small, and satisfy

$$Pr(l_u > 0) \approx Pr(B^r < 0) = \Phi\left(\frac{\mathrm{E}[B^r]}{\sqrt{\mathrm{Var}[B^r]}}\right), \tag{12}$$

$$Pr(l_o > 0) \approx Pr(B^r > C) = \Phi\left(\frac{C - \mathrm{E}[B^r]}{\sqrt{\mathrm{Var}[B^r]}}\right), \tag{13}$$

where Φ is the standard normal CDF.

We evaluate the accuracy of this approximation for a leakage queue with a Gaussian drift by comparing Equations (12) and (13) with simulations of the leakage queue. For the simulations,

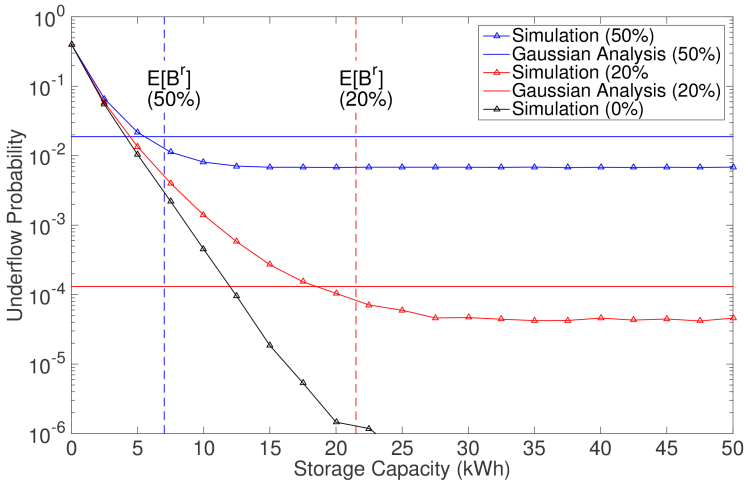

(a) Energy Loss (Underflow).

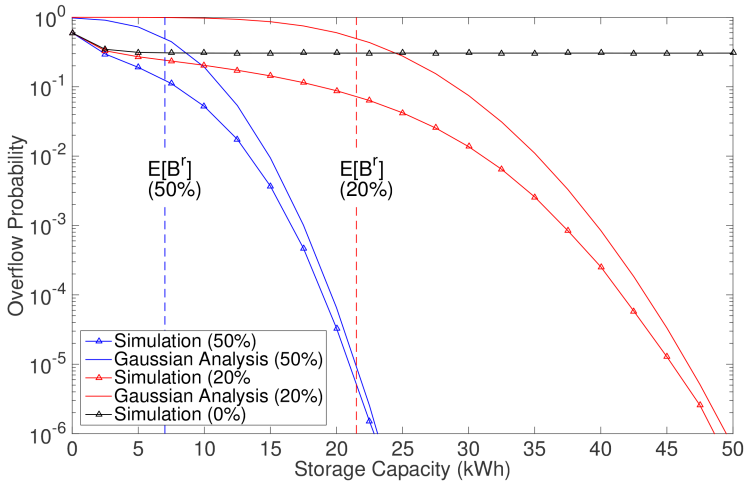

(b) Energy Waste (Overflow).

Fig. 6. Underflow and overflow of the leakage queue with Gaussian drift ($\mathrm{E}[a] = 1$ kWh, $\mathrm{E}[s] = 0.8$ kWh, $\sigma_a = 0.8$ kWh, $\sigma_s = 0.05$ kWh. The self-discharge per day is 0%, 20%, or 50%).

we compute averages over multiple repetitions of long simulation runs. We consider a storage system with a size up to 50 kWh, which covers a reasonable range for residential energy storage systems [53]. We assume a self-discharge of 20% per day ($\gamma = 0.0093$) or 50% per day ($\gamma = 0.0285$), and also consider a system without self-discharge ($\gamma = 0$). The energy supply and demand in a time slot of one hour are both Gaussian with expected values $\mathrm{E}[a] = 1$ kWh and $\mathrm{E}[s] = 0.8$ kWh, and standard deviations $\sigma_a = 0.8$ kWh and $\sigma_s = 0.05$ kWh. The resulting drift is Gaussian with $E[\delta] = \mathrm{E}[a] + \mathrm{E}[s]$ and variance $\mathrm{Var}[\delta] = \mathrm{Var}[a] + \mathrm{Var}[s]$.

Figure 6(a) depicts the underflow probability computed from Equation (12) as a function of the storage capacity and compares it with simulations. Since the expression for $Pr(B^r < 0)$ in Equation (12) does not depend on C, the analysis yields a straight line. The simulations of a system without leakage show that the underflow probability decreases exponentially in C. For systems

with leakage, however, the underflow probability becomes eventually constant in the leakage-dominated region ($C > \mathrm{E}[B^r]$). Increasing the storage capacity further does not reduce the underflow probability.

In Figure 6(b), we consider the energy wasted due to overflows. For the system without leakage, the overflow probability quickly settles at a value that does not depend on the storage capacity. Here, the storage is mostly full and the overflow compensates for the excess supply compared to the demand. With non-zero leakage, we observe a dramatically different behavior. The analytical estimate for $Pr(l_o > 0)$ from Equation (13) decreases faster than exponentially in C, which is also reflected in the simulations. We conclude that in leakage queues the overflow probability can be reduced arbitrarily by increasing the storage capacity.

Both plots in Figure 6 show that the Gaussian analysis can provide good estimates of the underflow and overflow probabilities when the system is in the leakage-dominated regime ($C > \mathrm{E}[B^r]$). Even if $\delta(n)$ does not follow a Gaussian distribution, the Gaussian analysis provides good estimates (see Section 6.1).

To understand why this is the case, let us consider general supply and demand processes that are i.i.d. with arbitrary distributions. By Equation (9), the stored energy B^r in the steady state of the reference system is the sum of independent random variables $\bar{\gamma}^m \delta(m)$. In the limit $\gamma \to 0$, these random variables become i.i.d. In analogy with the Central Limit Theorem, one should expect that the distribution of B^r approaches a Gaussian. The following result states that a suitably normalized version of B^r does converge to the standard normal distribution.

Theorem 5.1. *Let $\delta(n)$ be a sequence of i.i.d. random variables with finite mean and variance. For $0 < \gamma < 1$, let B^r be given by Equation (9). Then, as $\gamma \to 0$,*

$$Z := \frac{B^r - \mathrm{E}[B^r]}{\sqrt{\mathrm{Var}[B^r]}}$$

converges in distribution to a standard normal random variable.

Proof. It suffices to show that the characteristic function $\mathrm{E}[e^{i\theta Z}]$ converges to $e^{-\theta^2/2}$, the characteristic function of the standard normal distribution, for every $\theta \in \mathbb{R}$ [18, Theorem 3.3.6]. Let $\mathcal{X}(\theta)$ be the characteristic function of the normalized random variable $\frac{\delta - \mathrm{E}[\delta]}{\sqrt{\mathrm{Var}[\delta]}}$. By the i.i.d. assumption,

$$\mathrm{E}[e^{i\theta Z}] = \prod_{k=0}^{\infty} \mathcal{X}\left(\bar{\gamma}^k (1-\bar{\gamma}^2)^{\frac{1}{2}} \theta\right).$$

Since δ has finite variance, $\mathcal{X}$ is twice differentiable at zero, with $\mathcal{X}(0) = 1$, $\mathcal{X}'(0) = 0$, and $\mathcal{X}''(0) = 1$. Using the Taylor expansion of $\mathcal{X}$ about zero, a routine estimate for the product (see, for example, Reference [18, Exercise 3.1.1]) shows that $\mathrm{E}[e^{i\theta Z}] \to e^{-\theta^2/2}$ as $\gamma \to 0$. □

If γ is not close to zero, additional moments of B^r may be used to approximate its distribution. Since B^r is a sum of independent random variables, each of its cumulants can be computed directly from the corresponding cumulant of δ, using Equation (9). In particular, the skewness of B^r is given by

$$\mathrm{Skew}[B^r] = \frac{(1-\bar{\gamma}^2)^{\frac{3}{2}}}{1-\bar{\gamma}^3} \mathrm{Skew}[\delta]. \tag{14}$$

For non-zero skewness, a skew-normal distribution fitted to the mean, variance, and skewness of B^r provides a better approximation to $Pr(B^r > C)$ and $Pr(B^r < 0)$ than a Gaussian [4]. This approximation can be inserted in place of the Gaussian on the right-hand sides of Equation (12) and Equation (13). We will take advantage of the skew-normal approximation in Section 6.1.

5.2 Martingale Analysis

We have seen that the Gaussian analysis from the previous subsection provides a good level of accuracy in the leakage-dominated regime, but much less so in the capacity-dominated regime. A leakage queue in this regime is analogous to a finite capacity queueing system in overload. In this subsection, we prove bounds on the probability of underflow in the capacity-dominated regime. (The overflow probability is of less interest in this regime, since the stored energy is typically near capacity.)

There is extensive work in the literature on bounding the probability of buffer overflow in stable queueing systems [33]. An important tool is the *exponential martingale* technique, originally developed for studying hitting times of random walks and Brownian motion with drift [18, Exercises 5.7.4–5.7.9]. It has been used in the proof of the Kingman–Ross delay bounds [32, 45], as well as more complex situations including multiple queues [5], Markov-modulated processes [17, Section 3], and fork-join networks [44]. In those applications, the exponential martingale is applied to processes with stationary increments.

Q3

In our analysis, we use that underflows in the leakage queue correspond to overflows in the dual system presented in Section 3.2. The dual system is analogous to a stable queueing system in underload. We apply the exponential martingale associated with the random variable $\sum_{k=0}^{n} \bar{\gamma}^k \delta(k)$ to bound the overflow probability in the dual system. Different from the classical applications described above, the increments $\bar{\gamma}^k \delta(k)$ are not stationary for $0 < \gamma < 1$, requiring new ideas in the analysis that result in stronger bounds. When $\gamma = 0$, our bounds reduce to the classical ones.

Following is the main result of this subsection:

Theorem 5.2. *Consider a leakage queue with leakage ratio $0 < \gamma < 1$ and a drift given by an i.i.d. process $\delta(n)$. Assume that the moment-generating function $M(\theta) = \mathrm{E}[e^{\theta\delta}]$ is finite for at least some $\theta < 0$, and let*

$$\theta_0' := \sup\{\theta \geq 0 \mid \gamma\theta C + \log M(-\theta) \leq 0\},$$
$$\theta_1' := \sup\{\theta \geq 0 \mid \log M(-\theta) \leq 0\}.$$

In the capacity-dominated regime where $\gamma C < \mathrm{E}[\delta]$, we have $\theta_0' > 0$, and the underflow probability in the steady-state is bounded by

$$\log Pr(l_u > 0) \leq \frac{1}{|\log \bar{\gamma}|} \left\{ -\gamma\theta_0' C + \int_{\theta_0'}^{\theta_1'} \frac{\log M(-\tau)}{\tau}\, d\tau \right\}. \tag{15}$$

The proof of the theorem proceeds by bounding the *overflow* probability of the dual leakage queue introduced in Section 3.2, using the following two lemmas. The first lemma provides a basic bound on the probability of overflow.

Lemma 5.3. *Consider a leakage queue with leakage ratio $0 < \gamma < 1$ and a drift given by an i.i.d. process $\delta(n)$, whose expectation may be positive, negative, or zero. Assume that the moment-generating function $M(\theta) = \mathrm{E}[e^{\theta\delta}]$ is finite for some $\theta > 0$, and let*

$$\theta_0 = \sup\{\theta \geq 0 : \log M(\theta) \leq 0\}. \tag{16}$$

Then for every $\theta > 0$, the overflow probability in the steady state is bounded by

$$Pr(l_o > 0) \leq e^{-\theta C} \prod_{k \geq 0:\ \bar{\gamma}^k \theta > \theta_0} M(\bar{\gamma}^k \theta). \tag{17}$$

Proof. By Theorem 4.1, the steady-state of a leakage queue does not depend on the choice of the initial condition. Suppose the leakage queue is started with $B(0) = 0$. By Theorem 3.1, we have

for every $n > 0$,

$$\begin{aligned} B(n) &= \min_{0\le m\le n}\left\{\max_{m\le j\le n}\{\bar{\gamma}^{n-m}C\mathbb{1}_{j=m>0} + \Delta_\gamma(j,n)\}\right\} \\ &\le \max_{0\le j\le n}\{\Delta_\gamma(j,n)\} \\ &=_{\mathcal{D}} \max_{0\le m\le n}\left\{\sum_{k=0}^{m-1}\bar{\gamma}^k\delta(k)\right\}. \end{aligned}$$

In the second line, we have set $m = 0$, and in the third line, we have used the i.i.d. assumption. Taking $n \to \infty$ yields for the steady state

$$Pr(l_o > 0) \le Pr\left(\max_{m\ge 0}\sum_{k=0}^{m}\bar{\gamma}^k\delta(k) > C\right).$$

To derive a bound on the right-hand side, fix $\theta > 0$ and define the *exponential martingale* by the recursion

$$Z(0) = \frac{e^{\theta\delta(0)}}{M(\theta)}, \qquad Z(m) = \frac{e^{\bar{\gamma}^m\theta\delta(m)}}{M(\bar{\gamma}^m\theta)}Z(m-1), \quad (m > 0).$$

Since $\delta(m)$ is independent of $Z(m-1)$, the martingale property $\mathrm{E}[Z(m)|Z(m-1)] = Z(m-1)$ holds by construction. Solving the recursion yields

$$Z(m) = \frac{e^{\sum_{k=0}^{m}\bar{\gamma}^k\theta\delta(k)}}{\prod_{k=0}^{m}M(\bar{\gamma}^k\theta)}.$$

For $n \ge 0$, let t_n be the minimum of n and the first time slot when $\sum_{k=0}^{m}\bar{\gamma}^k\delta(k)$ exceeds C. By definition, $l_o > 0$ if and only if $t_n < n$ for some n. By the optional stopping theorem,

$$1 \;=\; \mathrm{E}[Z(0)] \;=\; \sum_{m=0}^{n}\mathrm{E}[Z(t_n)|t_n = m]\,Pr(t_n = m). \tag{18}$$

Clearly, $\sum_{k=0}^{m}\bar{\gamma}^k\delta(k) > C$ whenever $t_n = m < n$, and therefore,

$$\mathrm{E}[t_n|t_n = m] \;\ge\; \frac{e^{\theta C}}{\prod_{k=0}^{m}M(\bar{\gamma}^k\theta)}, \qquad (m < n).$$

Since the last summand in Equation (18) is nonnegative, it follows that

$$\begin{aligned} 1 &\ge \sum_{m=0}^{n-1}\mathrm{E}[Z(t_n)|t_n = m]\,Pr(t_n = m) \\ &\ge \frac{e^{\theta C}}{\prod_{k=0}^{\infty}\max\{M(\bar{\gamma}^k\theta), 1\}}Pr(t_n < n). \end{aligned}$$

We solve for $Pr(t_n < n)$ and take $n \to \infty$ to obtain

$$\begin{aligned} Pr(l_o \ge C) &\le \lim_{n\to\infty} Pr(t_n < n) \\ &\le e^{-\theta C}\prod_{k=0}^{\infty}\max\{M(\bar{\gamma}^k\theta), 1\}. \end{aligned}$$

The proof is completed by noting that $M(\bar{\gamma}^k\theta) \le 1$ for $\bar{\gamma}^k\theta < \theta_0$, and $M(\bar{\gamma}^k\theta) \ge 1$ otherwise. □

In Theorem 5.2, if $\mathrm{E}[\delta] < 0$, then we have $\theta_0 > 0$. Setting $\theta = \theta_0$ in Equation (17) then yields the bound

$$Pr(l_o > 0) \leq e^{-\theta_0 C}.$$

Note that this bound does not depend on γ, while the actual overflow probability decreases with γ. To capture this decrease, we next replace the bound on the overflow probability in Equation (17) by an expression that can be more easily computed in practice and then optimize over the choice of θ. The result is given by the following lemma.

Lemma 5.4. *Under the assumptions of Lemma 5.3, let*

$$\theta_1 = \sup\{\theta \geq 0 \mid \log M(\theta) \leq \gamma\theta C\}. \tag{19}$$

Then

$$\log Pr(l_o > 0) \leq \frac{1}{|\log \bar{\gamma}|} \left\{ -\gamma\theta_1 C + \int_{\theta_0}^{\theta_1} \frac{\log M(\tau)}{\tau}\, d\tau \right\}.$$

Proof. Taking logarithms in Equation (17) yields for any $\theta > 0$

$$\log Pr(l_o \geq C) \leq -\theta C + \sum_{k=0}^{\infty} [\log M(\theta\bar{\gamma}^k)]^+. \tag{20}$$

We next use the convexity of the function $[\log M(\theta)]^+$ to replace the sum by an integral. For any $\theta > 0$, the density $\rho(\tau) = (\tau|\log\bar{\gamma}|)^{-1}$ defines a probability measure with mean θ on the interval

$$I(\theta) := \left\{ \tau \,\middle|\, \bar{\gamma}|\log\bar{\gamma}|\theta \leq \gamma\tau < |\log\bar{\gamma}|\theta \right\}.$$

Indeed, one easily checks that

$$\int_{I(\theta)} \frac{1}{\tau|\log\bar{\gamma}|}\, d\tau = 1, \qquad \int_{I(\theta)} \frac{\tau}{\tau|\log\bar{\gamma}|}\, d\tau = \theta.$$

By Jensen's inequality,

$$[\log M(\theta)]^+ \leq \int_{I(\theta)} \frac{[\log M(\tau)]^+}{\tau|\log\bar{\gamma}|}\, d\tau,$$

and correspondingly for $\bar{\gamma}^k\theta$ in place of θ. Since the intervals $I(\bar{\gamma}^k\theta)$ are disjoint for $k \geq 0$, and their union is given by

$$\bigcup_{k\geq 0} I(\bar{\gamma}^k\theta) = \{\tau \mid 0 < \gamma\tau < |\log\bar{\gamma}|\theta\},$$

it follows that

$$\sum_{k=0}^{\infty} [\log M(\bar{\gamma}^k\theta)]^+ \leq \frac{1}{|\log\bar{\gamma}|} \int_0^{\gamma^{-1}|\log\bar{\gamma}|\theta} \frac{[\log M(\tau)]^+}{\tau}\, d\tau.$$

We then insert this estimate into Equation (20), replace θ with $\gamma(|\log\bar{\gamma}|)^{-1}\theta$, and use that $\log M(\tau) \leq 0$ for $0 \leq \tau \leq \theta_0$ and positive otherwise to obtain

$$\log Pr(l_o > 0) \leq \frac{1}{|\log\bar{\gamma}|} \left\{ -\gamma\theta C + \int_{\theta_0}^{\theta} \frac{\log M(\tau)}{\tau}\, d\tau \right\}.$$

The right-hand side achieves its minimum at $\theta = \theta_1$. □

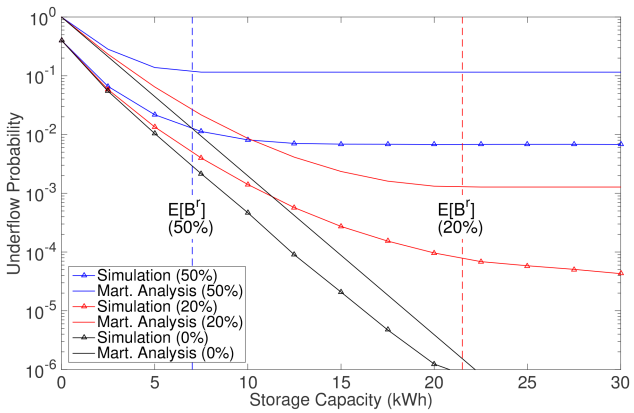

Fig. 7. Underflow of the leakage queue in the capacity-dominated regime. (E[a] = 1 kWh, E[s] = 0.8 kWh, σ_a = 0.8 kWh, σ_s = 0.05 kWh. The self-discharge per day is 0%, 20%, or 50%).

Proof of Theorem 5.2. Consider the dual leakage queue defined in Section 3.2, with drift process $\delta'(n) = \gamma C - \delta(n)$. By assumption, its moment-generating function $M'(\theta) = e^{\gamma\theta C} M(-\theta)$ is finite for some $\theta > 0$. Therefore, we can apply Lemma 5.4 to the dual leakage queue. By definition,

$$\theta_0' = \sup\{\theta \geq 0 : \log M'(\theta) \leq 0\},$$
$$\theta_1' = \sup\{\theta \geq 0 : \log M'(\theta) \leq \gamma\theta C\}$$

(see Equations (16) and (19)). It follows from Lemma 5.4 that

$$\log Pr(l_u > 0) = \log Pr(l_o' > 0)$$
$$\leq \frac{1}{|\log \bar{\gamma}|} \left\{ -\gamma\theta_1' C + \int_{\theta_0'}^{\theta_1'} \frac{\log M'(\tau)}{\tau}\, d\tau \right\}.$$

Since $\log M'(\theta) = \gamma\theta C + \log M(-\theta)$, this proves the claim. □

We note that Theorem 5.2, Lemma 5.3, and Lemma 5.4 remain valid in the leakage-dominated regime. In that regime, $\theta_0 = \theta_0' = 0$, but θ_1 and θ_1' are positive, resulting in non-trivial bounds on the probabilities of overflow and underflow.

Example. If δ is Gaussian, the bounds on the overflow and underflow probabilities can be evaluated in closed form, as follows: Suppose δ has mean E[δ] = $\mu > 0$ and variance Var[δ] = σ^2. Using that $\log M(\theta) = \mu\theta + \frac{\sigma^2}{2}\theta^2$, we compute $\theta_0 = 0$, $\theta_1 = \frac{2}{\sigma^2}[\gamma C - \mu]^+$, $\theta_0' = \frac{2}{\sigma^2}[\mu - \gamma C]^+$, and $\theta_1' = \frac{2\mu}{\sigma^2}$. The resulting bounds are:

- **Capacity-dominated regime ($\gamma C \leq \mu$):**

$$Pr(l_u > 0) \leq e^{-\frac{(\gamma C)(2\mu - \gamma C)}{|\log \bar{\gamma}|\sigma^2}}.$$

- **Leakage-dominated regime ($\gamma C > \mu$):**

$$Pr(l_u > 0) \leq e^{-\frac{\mu^2}{|\log \bar{\gamma}|\sigma^2}}, \quad Pr(l_o > 0) \leq e^{-\frac{(\gamma C - \mu)^2}{|\log \bar{\gamma}|\sigma^2}}.$$

In Figure 7, we evaluate the underflow probabilities obtained with Theorem 5.2 for a leakage queue with Gaussian supply and demand processes as in Section 5.1, with the same set of parameters. The martingale bounds provide good upper bounds on the underflow probabilities in the

Table 1. Parameters of the Wind Turbine

Notation	Definition	value
P_r	Rated power	1 kW
v_{ci}	Cut-in wind speed	3 m/s
v_{co}	Cut-out wind speed	25 m/s
v_r	Rated wind speed	12 m/s
A_w	Total swept area	10.8 m^2
η_w	Wind turbine efficiency	50%

capacity-dominated regime (to the left of the respective value of $E[B^r]$). In the leakage-dominated regime, the bounds are less accurate than the Gaussian analysis in Figure 6(a).

6 EVALUATION WITH A WIND ENERGY MODEL

We next consider a leakage queue with a supply process that resembles a wind energy source. Our objectives are twofold. First, we want to see if the reference system remains useful in the context of more complex random processes. Second, we want to evaluate the accuracy of our analysis. We use the wind speed process from Reference [48], which models wind speed as an i.i.d. process with a Weibull distribution with density function

$$f_V(v) = \frac{k}{c}\left(\frac{v}{c}\right)^{k-1} e^{-\left(\frac{v}{c}\right)^k},$$

where c and k, respectively, are the scale and shape parameters of the Weibull distribution. As in Reference [48], we set the shape parameter to $k = 3$. The scale parameter factor is set to $c = 7$ m/s, which results in an average wind speed of 6.25 m/s.

We consider a wind turbine with a rated power of $P_r = 1$ kW, which is comparable to a micro wind turbine for a residential home [7]. The output power of wind turbines, denoted by P_w and expressed in kW/m^2, is a function of the wind speed v. Wind turbines are activated only when the wind speed is above a lower threshold (cut-in speed) and below an upper threshold (cut-out speed). The rated speed is the wind speed at which the wind turbine generates its rated power P_r. Using the power model from Reference [10], we obtain

$$P_w = \begin{cases} 0 & v < v_{ci}, \\ \alpha v^3 - \beta P_r & v_{ci} \le v \le v_r, \\ P_r & v_r \le v \le v_{co}, \\ 0 & v_{co} \le v, \end{cases} \tag{21}$$

where v_{ci}, v_r and v_{co}, respectively, are the cut-in, rated, and cut-out wind speeds, and α and β are calculated such that Equation (21) is continuous at v_{ci} and v_r, i.e., $\alpha = \frac{P_r}{v_r^3 - v_{ci}^3}$ and $\beta = \frac{v_{ci}^3}{v_r^3 - v_{ci}^3}$. The actual power from the wind turbine is given by [10]

$$a(n) = P_w \cdot A_w \cdot \eta_w,$$

where A_w and η_w are the total swept area and the efficiency of the wind turbine, respectively. The parameters of the wind turbine are summarized in Table 1. With these parameters, we obtain a supply process with $\mathrm{E}[a] = 1$ kWh and $\sigma_a = 1.05$ kWh.

The demand process is set as the sum of a constant demand of 0.75 kWh and an i.i.d. exponential random value with average 0.05 kWh, resulting in $\mathrm{E}[s] = 0.8$ kWh and $\sigma_s = 0.05$ kWh. We consider energy storage systems with a significant self-discharge, with leakage ratios $\gamma = 0.0093$

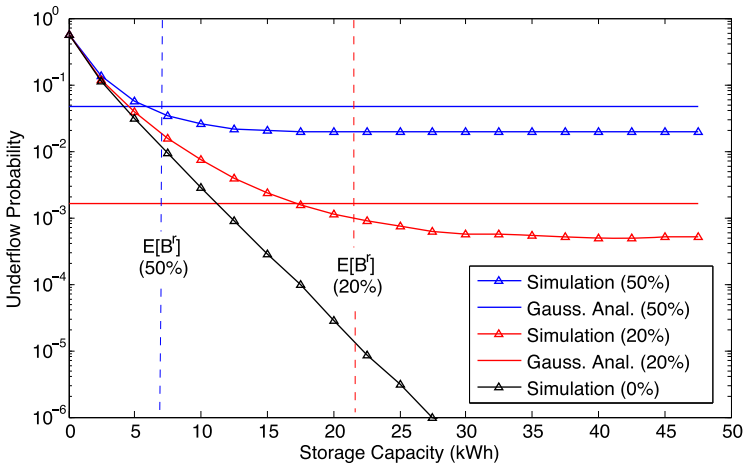

(a) Energy Loss (Underflow).

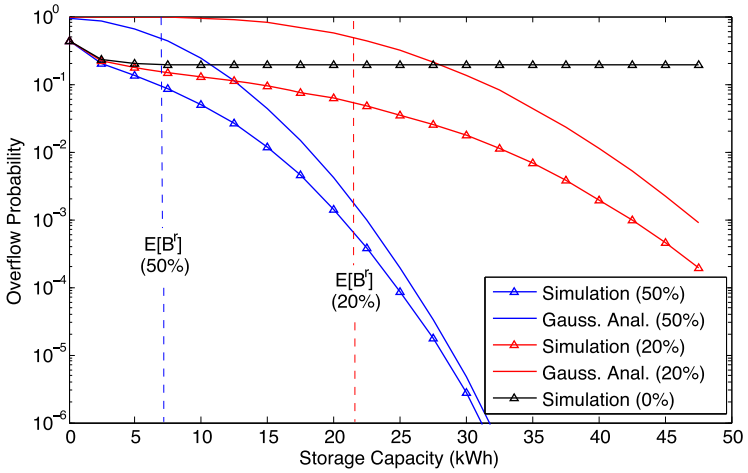

(b) Energy Waste (Overflow).

Fig. 8. Underflow and overflow probabilities of the leakage queue with wind energy source. ($\mathrm{E}[a] = 1$ kWh, $\mathrm{E}[s] = 0.8$ kWh, $\sigma_a = 1.05$ kWh, $\sigma_s = 0.05$ kWh. The self-discharge per day is 0%, 20%, or 50%).

(20% per day) and $\gamma = 0.0285$ (50% per day), which is within the range of supercapacitors or flywheels. As before, we use 1 hour for the length of a time slot.

6.1 Underflow and Overflow Probabilities

In Figure 8, we show the underflow and overflow probability as a function of the capacity C for different leakage ratios. We compare the results of the Gaussian analysis with simulations. Note that the average drift $E[\delta]$ as well as the leakage ratios match the examples in Section 5. A comparison of Figure 8 with Figure 6 validates the Gaussian analysis for supply and demand distributions that are not Gaussian.

Figure 8 shows that the accuracy of the Gaussian analysis is high in the leakage-dominated regime ($C > \mathrm{E}[B^r]$). As seen in Figure 6 for Gaussian supply and demand, the underflow probability

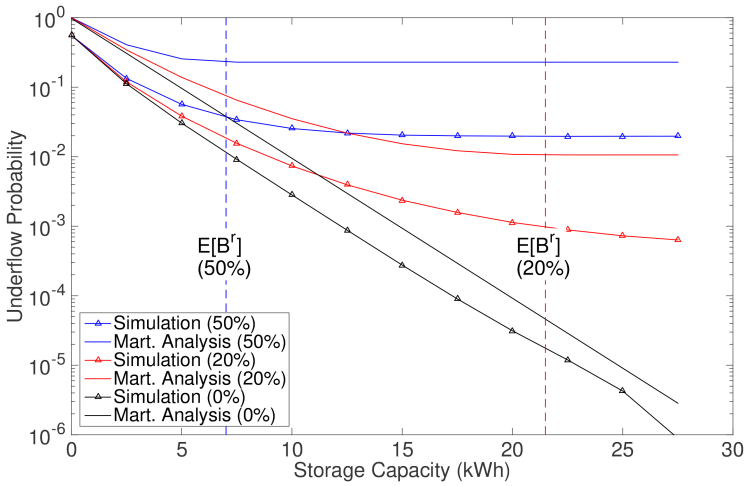

Fig. 9. Underflow probability of the leakage queue with wind energy source in the capacity-dominated regime. ($\mathrm{E}[a] = 1$ kWh, $\mathrm{E}[s] = 0.8$ kWh, $\sigma_a = 1.05$ kWh, $\sigma_s = 0.05$ kWh. The self-discharge per day is 0%, 20%, or 50%).

(Figure 8(a)) approaches a constant when the capacity is increased. For the overflow probability (Figure 8(b)), we again observe a faster than exponential decay in C in the presence of leakage.

In Figure 9, we present the underflow probabilities computed with the martingale analysis, which extends to the capacity-dominated regime. Here, the underflow probabilities decreases more slowly in the storage capacity, as compared to a conventional system without leakage. Once the system approaches the leakage-dominated regime, increasing the buffer size has a negligible impact on the underflow probability.

6.2 Another Validation of the Reference System

We return to the main finding of this article, which is the distinct behavior of the leakage queue in the leakage-dominated regime. In Section 3.3, we used empirical data to show that the reference system provides an accurate characterization of the leakage queue. Further, in Section 5.1, we proved for this regime that the reference system approaches a Gaussian distribution when γ is small. Next, we compare the distribution of the stored energy (backlog) in the leakage queue with a Gaussian distribution.

We work with the same supply and demand processes as before. We consider energy storage systems with $\gamma = 0.0093$ (20% self-discharge per day), and, therefore, $\mathrm{E}[B^r] = 21.5$ kWh. The queue is leakage-dominated for $C = 40$ kWh and capacity-dominated for $C = 10$ kWh and $C = 20$ kWh.

The distributions of the stored energy are presented in a quantile-quantile (Q-Q) plot. We compare quantiles of simulations of a leakage queue with those of the Gaussian distribution. In Figure 10, we provide the quantiles of the Gaussian distribution on the horizontal axis. The diagonal line, shown as a thin solid line, therefore, depicts the Gaussian distribution. The thick solid line (in gray) has the results for the skew-normal distribution, using the skewness for B^r from Equation (14). The quantiles obtained from the simulations are shown as colored data points in increments of 5%. The closer the data points are to the diagonal, the better the match is with the Gaussian distribution. We observe that the stored energy in a leakage-dominated regime ($C = 40$ kWh) is very close to the diagonal. The match is further improved with the skew-normal distribution. The capacity-dominated regime ($C = 10, 20$ kWh) is obviously poorly matched with a Gaussian

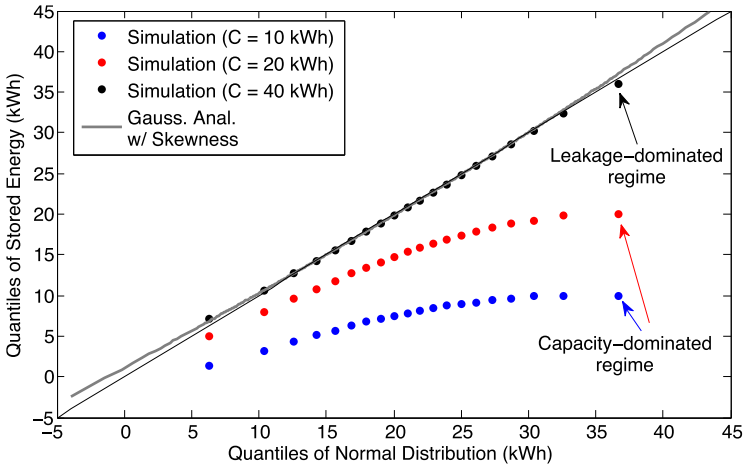

Fig. 10. Distribution of the stored energy (backlog) for the leakage queue with wind energy source. (Self-discharge per day is 20%; $C = 10, 20, 40$ kWh, $\mathrm{E}[a] = 1$ kWh, $\mathrm{E}[s] = 0.8$ kWh, $\sigma_a = 1.05$ kWh, $\sigma_s = 0.05$ kWh).

distribution. Even, for $C = 20$ kWh, when the storage capacity is close to $\mathrm{E}[B^r]$, the Q-Q plot is far from the diagonal.

7 CONCLUSIONS

We presented an analysis of a queueing model for an energy storage system with self-discharge. The model, referred to as *leakage queue*, has a self-discharge process that removes storage content proportionally to the filling level. We identified two distinct parameter regimes for the leakage queue, which we called leakage-dominated regime and capacity-dominated regime. In the leakage-dominated regime, the queue settles in a steady state below the storage capacity. In the capacity-dominated regime, the leakage queue resembles a conventional finite capacity queueing system. We presented analytical methods for computing probabilities of underflow and overflow and evaluated their accuracy. An extension of our work is a relaxation of the i.i.d. assumption to general stationary arrival and service processes. For the leakage-dominated regime, a natural approach will be to establish a reference system using a Gaussian process with autocorrelations. For the capacity-dominated regime, an extension could benefit from the recent martingale analysis of a finite capacity queue with Markov-modulated arrivals by Ciucu, Poloczek, and Rizk. However, that analysis can currently not account for a leakage process as considered in this article.

APPENDICES

A PROOF OF LEMMA 4.2

Proof. For the first claim, we use that the CDF of αX_i is

$$Pr(\alpha X_i \le x) = F_i(\alpha^{-1}x), \quad i = 1, 2$$

and compute

$$\begin{aligned} d(\gamma X_1, \gamma X_2) &= \int_{-\infty}^{\infty} |F_1(\alpha^{-1}x) - F_2(\alpha^{-1}x)|\, dx \\ &= \alpha \int_{-\infty}^{\infty} |F_1(y) - F_2(y)|\, dy \\ &= \alpha\, d(X_1, X_2). \end{aligned}$$

The next two claims are immediate from the facts that the CDF of $[X_i]^+$ is $F_i \mathbb{1}_{x>0}$, and the CDF of $\min\{X_i, C\}$ is $F_i \mathbb{1}_{x \leq C}$. For the final claim, let μ be the probability distribution of Y. Then the CDF of $X_i + Y$ is $F_i * \mu(x) = \int F_i(x-y)\, d\mu(y)$ for $i = 1, 2$. Therefore,

$$\begin{aligned} d(X_1 + Y, X_2 + Y) &= \int_{-\infty}^{\infty} \left| \int_{-\infty}^{\infty} F_1(x-y) - F_2(x-y)\, d\mu(y) \right| dx \\ &\leq \int_{-\infty}^{\infty} \int_{-\infty}^{\infty} \left| F_1(x-y) - F_2(x-y) \right| d\mu(y)\, dx \\ &= d(X_1, X_2). \end{aligned}$$

We have used Minkowski's inequality and then applied Fubini's theorem. □

B PROOF OF COROLLARY 4.4

Proof. By Theorem 4.1, the distribution of the stored energy $B(n)$ in the leakage queue converges to the steady state regardless of the choice of the initial condition $B(0)$. Let us use the steady state of the reference system as an initial condition for $B(n)$, that is, $B(0) =_{\mathcal{D}} B^r$. It is a consequence of the contraction mapping theorem that the distance to the steady state is bounded by

$$d(B, B(n)) \leq \frac{\bar{\gamma}^n}{\gamma}\, d(B(1), B(0)).$$

We set $n = 0$ and proceed to estimate $d(B(1), B(0))$. Due to our choice of the initial state, Equation (1) yields

$$B(1) =_{\mathcal{D}} \Psi(B) = \min\left\{[B]^+, C\right\},$$

because $\bar{\gamma} B^r + \delta =_{\mathcal{D}} B^r$ by the definition of the reference system. Therefore,

$$d(B(1), B(0)) = \int_{-\infty}^{0} Pr(B^r \leq x)\, dx + \int_{C}^{\infty} Pr(B^r > x)\, dx,$$

completing the proof. □

REFERENCES

[1] C. J. Ancker Jr. and A. V. Gafarian. 1963. Some queuing problems with balking and reneging, I. *Oper. Res.* 11, 1 (Jan./Feb. 1963), 88–100.
[2] O. Ardakanian, S. Keshav, and C. Rosenberg. 2012. On the use of teletraffic theory in power distribution systems. In *Proceedings of the 3rd International Conference on Energy-efficient Computing and Networking (ACM e-Energy'12)*. 1–10.
[3] S. Athuraliya, S. H. Low, V. Li, and Q. Yin. 2001. REM: Active queue management. *IEEE Netw.* 15, 3 (2001), 48–53.
[4] A. Azzalini. 2013. *The Skew-normal and Related Families*. Cambridge University Press.
[5] F. Baccelli. 1986. Exponential martingales and Wald's formulas for two-queue networks. *J. Appl. Probab.* 23, 3 (1986), 812–819.
[6] F. Baccelli, P. Boyer, and G. Hebuterne. 1984. Single-server queues with impatient customers. *Adv. Appl. Probab.* 16, 4 (1984), 887–905.
[7] A. . Bahaj, L. Myers, and P. A. B. James. 2007. Urban energy generation: Influence of micro-wind turbine output on electricity consumption in buildings. *Energy Build.* 39, 2 (2007), 154–165.
[8] N. Barjesteh. 2013. *Duality Relations in Finite Queueing Models*. Master's Thesis. University of Waterloo, Canada. Retrieved from http://hdl.handle.net/10012/7715.
[9] O. Boxma and B. Zwart. 2018. Fluid flow models in performance analysis. *Comput. Commun.* 131 (2018), 22–25.
[10] R. Chedid, H. Akiki, and S. Rahman. 1998. A decision support technique for the design of hybrid solar-wind power systems. *IEEE Trans. Energy Convers.* 13, 1 (1998), 76–83.
[11] M. Chen and G. A. Rincon-Mora. 2006. Accurate electrical battery model capable of predicting runtime and IV performance. *IEEE Trans. Energy Convers.* 21, 2 (2006), 504–511.
[12] F. Ciucu, F. Poloczek, and A. Rizk. 2019. Queue and loss distributions in finite-buffer queues. *Proc. ACM Meas. Anal. Comput. Syst.* 3, 2 (June 2019), 31:1–31:29.
[13] J. W. Cohen. 1969. *The Single Server Queue*. North-Holland.

[14] R. L. Cruz and H. N. Liu. 1993. Single server queues with loss: A formulation. In *Proceedings of the Conference on Information Sciences and Systems (CISS'93)*. John Hopkins University.
[15] A. Dekka, R. Ghaffari, B. Venkatesh, and B. Wu. 2015. A survey on energy storage technologies in power systems. In *Proceedings of the IEEE Electrical Power and Energy Conference (EPEC'15)*. 105–111.
[16] K. C. Divya and J. Østergaard. 2009. Battery energy storage technology for power systems—An overview. *Electr. Pow. Syst. Res.* 79, 4 (2009), 511–520.
[17] N. Duffield. 1994. Exponential bounds for queues with Markovian arrivals. *Queue. Syst.* 17, 3–4 (1994), 413–430.
[18] R. Durrett. 2010. *Probability: Theory and Examples (4th Edition)*. Cambridge University Press.
[19] S. Floyd and V. Jacobson. 1993. Random early detection gateways for congestion avoidance. *IEEE/ACM Trans. Netw.* 1, 4 (1993), 397–413.
[20] D. Fooladivanda, G. Mancini, S. Garg, and C. Rosenberg. 2014. State of charge evolution equations for flywheels. *CoRR* abs/1411.1680 (Nov. 2014).
[21] D. Fooladivanda, C. Rosenberg, and S. Garg. 2016. Energy storage and regulation: An analysis. *IEEE Trans. Smart Grid* 7, 4 (2016), 1813–1823.
[22] L. Gelazanskas and K. Gamage. 2014. Demand side management in smart grid: A review and proposals for future direction. *Sustain. Cities Society* 11 (2014), 22–30.
[23] E. Gelenbe, P. Glynn, and K. Sigman. 1991. Queues with negative arrivals. *J. Appl. Probab.* 28, 1 (1991), 245–250.
[24] Y. Ghiassi-Farrokhfal, S. Keshav, and C. Rosenberg. 2015. Toward a realistic performance analysis of storage systems in smart grids. *IEEE Trans. Smart Grid*1 (2015), 402–410.
[25] Y. Ghiassi-Farrokhfal, C. Rosenberg, S. Keshav, and M. B. Adjaho. 2016. Joint optimal design and operation of hybrid energy storage systems. *IEEE J. Select. Areas Commun.* 34, 3 (Mar. 2016), 639–650.
[26] P. G. Harrison and E. Pitel. 1996. The M/G/1 queue with negative customers. *Adv. Appl. Probab.* 28, 2 (June 1996), 540–566.
[27] H. Ibrahim, A. Ilinca, and J. Perron. 2008. Energy storage systems–characteristics and comparisons. *Renew. Sustain. Energy Rev.* 12, 5 (2008), 1221–1250.
[28] D.-M. Chiu, R. Jain. 1989. Analysis of the increase and decrease algorithms for congestion avoidance in computer networks. *Comput. Netw.orks and ISDN Syst.* 17, 1 (1989), 1–14.
[29] G. L. Jones, P. G. Harrison, U. Harder, and T. Field. 2011. Fluid queue models of battery life. In *Proceedings of the IEEE 19th Annual International Symposium on Modelling, Analysis, and Simulation of Computer and Telecommunication Systems (MASCOTS'11)*. 278–285.
[30] F. Kazhamiaka, C. Rosenberg, S. Keshav, and K.-H. Pettinger. 2016. Li-ion storage models for energy system optimization: The accuracy-tractability tradeoff. In *Proceedings of the 7th International Conference on Future Energy Systems (ACM e-Energy'16)*. 17:1–17:12.
[31] F. P. Kelly. 1991. Effective bandwidths at multi-class queues. *Queue. Syst.ems* 9, 1–2 (1991), 5–15.
[32] J. F. C. Kingman. 1964. A martingale inequality in the theory of queues. *Math. Proc. Cambr. Philos. Society* 60, 2 (1964), 359–361.
[33] H. Kobayashi and A. Konheim. 1977. Queueing models for computer communications system analysis. *IEEE Trans. Commun.* 25, 1 (1977), 2–29.
[34] I. Koutsopoulos, V. Hatzi, and L. Tassiulas. 2011. Optimal energy storage control policies for the smart power grid. In *Proceedings of the International Conference on Communications, Control, and Computing Technologies for Smart Grids (IEEE SmartGridComm'11)*. 475–480.
[35] J. Y. Le Boudec and P. Thiran. 2001. *Network Calculus* (*Lecture Notes in Computer Science, Vol. 2050)*. Springer Verlag.
[36] J.-Y. Le Boudec and D.-C. Tomozei. 2012. A demand-response calculus with perfect batteries. In *Proceedings of the 16th International GI/ITG Conference (MMB & DFT), Workshop on Network Calculus (WoNeCa)*. Springer Berlin, 273–287.
[37] N. Li, L. Chen, and S. H. Low. 2011. Optimal demand response based on utility maximization in power networks. In *Proceedings of the IEEE Power and Energy Society General Meeting*. 1–8.
[38] Z. Liu, I. Liu, S. Low, and A. Wierman. 2014. Pricing data center demand response. In *Proceedings of the ACM SIGMETRICS International Conference on Measurement and Modeling of Computer Systems*. 111–123.
[39] A.-H. Mohsenian-Rad, V. W. S. Wong, J. Jatskevich, R. Schober, and A. Leon-Garcia. 2010. Autonomous demand-side management based on game-theoretic energy consumption scheduling for the future smart grid. *IEEE Trans. Smart Grid* 1, 3 (2010), 320–331.
[40] National Renewable Energy Laboratory. 1992. National Solar Radiation Data Base, 1961–1990: Typical Meteorological Year 2. Retrieved from http://rredc.nrel.gov/solar/old_data/nsrdb/1961-1990/tmy2/.
[41] National Renewable Energy Laboratory. 2017. System Advisor Model Version 2017.9.5 (SAM 2017.9.5). Retrieved from https://sam.nrel.gov/downloads.
[42] M. A. Pedrasa, T. D. Spooner, and I. F. MacGill. 2010. Coordinated scheduling of residential distributed energy resources to optimize smart home energy services. *IEEE Trans. Smart Grid* 1, 2 (2010), 134–143.

[43] R. M. Phatarfod. 1963. Application of methods in sequential analysis to dam theory. *Ann. Math. Statist.* 34, 4 (1963), 1588–1592.
[44] A. Rizk, F. Poloczek, and F. Ciucu. 2015. Computable bounds in fork-join queueing systems. In *Proceedings of the ACM SIGMETRICS International Conference on Measurement and Modeling of Computer Systems*. 335–346.
[45] S. M. Ross. 1974. Bounds on the delay distribution in GI/G/1 queues. *J. Appl. Probab.* 11, 2 (June 1974), 417–421.
[46] Z. M. Salameh, M. A. Casacca, and W. A. Lynch. 1992. A mathematical model for lead-acid batteries. *IEEE Trans. Energy Convers.* 7, 1 (1992), 93–98.
[47] P. Samadi, A.-H. Mohsenian-Rad, R. Schober, V. W. S. Wong, and J. Jatskevich. 2010. Optimal real-time pricing algorithm based on utility maximization for smart grid. In *Proceedings of the 1st IEEE International Conference on Communications, Control, and Computing Technologies for Smart Grids (SmartGridComm'10)*. 415–420.
[48] J. V. Seguro and T. W. Lambert. 2000. Modern estimation of the parameters of the Weibull wind speed distribution for wind energy analysis. *J. Wind Eng. Industr. Aerody.* 85, 1 (2000), 75–84.
[49] S. Singla, Y. Ghiassi-Farrokhfal, and S. Keshav. 2014. Using storage to minimize carbon footprint of diesel generators for unreliable grids. *IEEE Trans. Sustain. Energy* 5, 4 (2014), 1270–1277.
[50] H. I. Su and A. E. Gamal. 2013. Modeling and analysis of the role of energy storage for renewable integration: Power balancing. *IEEE Trans. Power Syst.* 28, 4 (2013), 4109–4117.
[51] S. Sun, M. Dong, and B. Liang. 2014. Real-time power balancing in electric grids with distributed storage. *IEEE J. Select. Topics Sig. Proc.* 8, 6 (2014), 1167–1181.
[52] S. Sun, B. Liang, M. Dong, and J. A. Taylor. 2016. Phase balancing using energy storage in power grids under uncertainty. *IEEE Trans. Power Syst.* 31, 5 (2016), 3891–3903.
[53] Tesla Inc. 2019. Tesla Powerwall. Retrieved from https://www.tesla.com/powerwall.
[54] C. Thrampoulidis, S. Bose, and B. Hassibi. 2016. Optimal placement of distributed energy storage in power networks. *IEEE Trans. Automat. Contr.* 61, 2 (2016), 416–429.
[55] D. Wang, C. Ren, A. Sivasubramaniam, B. Urgaonkar, and H. Fathy. 2012. Energy storage in datacenters: What, where, and how much? In *Proceedings of the ACM SIGMETRICS International Conference on Measurement and Modeling of Computer Systems*. 187–198.
[56] K. Wang, F. Ciucu, C. Lin, and S. H. Low. 2012. A stochastic power network calculus for integrating renewable energy sources into the power grid. *IEEE J. Select. Areas Commun.* 30, 6 (2012), 1037–1048.
[57] A. R. Ward. 2012. Asymptotic analysis of queueing systems with reneging: A survey of results for FIFO, single class models. *Surv. Oper. Res. Manag. Sci.* 17, 1 (2012), 1–14.
[58] World Energy Council. 2016. Energy Efficiency Indicators. Retrieved from https://wec-indicators.enerdata.net/household-electricity-use.html.
[59] K. Wu, Y. Jiang, and D. Marinakis. 2012. A stochastic calculus for network systems with renewable energy sources. In *Proceedings of the IEEE INFOCOM Workshops*. 109–114.
[60] P. Yang and A. Nehorai. 2014. Joint optimization of hybrid energy storage and generation capacity with renewable energy. *IEEE Trans. Smart Grid* 5, 4 (2014), 1566–1574.

Received November 2019; revised July 2020; accepted September 2020

Author Queries

Q1: AU: Please supply the CCS Concepts 2012 codes per the ACM style indicated on the ACM website. Please include the CCS Concepts XML coding as well.

Q2: AU: Please provide complete mailing addresses for all authors.

Q3: AU: "we use that underflows in the leakage queue correspond to overflows in the dual system presented in Section 3.2." written as meant?